



The Continuous Electron Beam Accelerator Facility  
Theory Group Preprint Series

Additional copies are available from the authors.

The Southeastern Universities Research Association (SURA) operates the Continuous Electron Beam Accelerator Facility for the United States Department of Energy under contract DE-AC05-84ER40150

Stranger Still: Kaon Loops and Strange Quark  
Matrix Elements of the Nucleon<sup>1</sup>

M. J. Musolf

*Department of Physics  
Old Dominion University  
Norfolk, VA 23529 U.S.A.*

and

*CEBAF Theory Group, MS-12H  
12000 Jefferson Ave.  
Newport News, VA 23606 U.S.A.*

and

M. Burkardt

*Center for Theoretical Physics  
Laboratory for Nuclear Science  
and Department of Physics  
Massachusetts Institute of Technology  
Cambridge, Massachusetts 02139 U.S.A.*

DISCLAIMER

This report was prepared as an account of work sponsored by the United States government. Neither the United States nor the United States Department of Energy, nor any of their employees, makes any warranty, express or implied, or assumes any legal liability or responsibility for the accuracy, completeness, or usefulness of any information, apparatus, product, or process disclosed, or represents that its use would not infringe privately owned rights. Reference herein to any specific commercial product, process, or service by trade name, mark, manufacturer, or otherwise, does not necessarily constitute or imply its endorsement, recommendation, or favoring by the United States government or any agency thereof. The views and opinions of authors expressed herein do not necessarily state or reflect those of the United States government or any agency thereof.

CEBAF #TH-93-01

January, 1993

<sup>1</sup>This work is supported in part by funds provided by the U. S. Department of Energy (D.O.E.) under contracts #DE-AC02-76ER03069 and #DE-AC05-84ER40150.

## ABSTRACT

Intrinsic strangeness contributions to low-energy strange quark matrix elements of the nucleon are modelled using kaon loops and meson-nucleon vertex functions taken from nucleon-nucleon and nucleon-hyperon scattering. A comparison with pion loop contributions to the nucleon electromagnetic (EM) form factors indicates the presence of significant SU(3)-breaking in the mean-square charge radii. As a numerical consequence, the kaon loop contribution to the mean square Sachs strangeness radius is significantly smaller than could be observed with parity-violating elastic  $\bar{\nu}p$  experiments planned for CEBAF, while the contribution to the Sachs radius is large enough to be observed with PV electron scattering from  $(0^+, 0)$  nuclei. Kaon loops generate a strange magnetic moment of the same scale as the isoscalar EM magnetic moment – a scale large enough to be observed at CEBAF – and a strange axial vector form factor having roughly one-third of the magnitude extracted from  $\nu p/\bar{\nu}p$  elastic scattering. In the chiral limit, the loop contribution to the fraction of the nucleon’s scalar density arising from strange quarks has roughly the same magnitude as the value extracted from analyses of  $\Sigma_{\pi N}$ . The importance of satisfying the Ward-Takahashi Identity, not obeyed by previous calculations, is also illustrated, and the sensitivity of results to input parameters is analyzed.

## 1. Introduction

Extractions of the strange quark scalar density from  $\Sigma_{\pi N}$  [1,2], the strange quark axial vector form factor from elastic  $\nu p/\bar{\nu}p$  cross section measurements [3], and the strange-quark contribution to the proton spin  $\Delta s$  from the EMC measurement of the  $g_1$  sum [4], suggest a need to account explicitly for the presence of strange quarks in the nucleon in describing its low-energy properties. These analyses have motivated suggestions for measuring strange quark vector current matrix elements of the nucleon with semi-leptonic neutral current scattering [5]. The goal of the SAMPLE experiment presently underway at MIT-Bates [6] and the “ $G^0$ ” experiment planned for CEBAF [8] is to constrain the strange quark magnetic form factor at low- $|q^2|$ , and three experiments have been planned at CEBAF with the objective of constraining the nucleon’s mean square “strangeness radius” [7-9]. In addition, a new determination of the strange quark axial vector form factor at significantly lower  $|q^2|$  than was obtained from the experiment of Ref. [3] is expected from LSND experiment at LANL [10].

At first glance, the existence of non-negligible low energy strange quark matrix elements of the nucleon is rather surprising, especially in light of the success with which constituent quark models account for other low-energy properties of the nucleon and its excited states. Theoretically, one might attempt to understand the possibility of large strange matrix elements from two perspectives associated, respectively, with the high- and low-momentum components of a virtual  $s\bar{s}$  pair in the nucleon. Contributions from the high-momentum component may be viewed as “extrinsic” to the nucleon’s wavefunction, since the lifetime of the virtual pair at high-momentum scales is shorter than the interaction time associated with the formation of hadronic states [11]. In an effective theory framework, the extrinsic, high-momentum contributions renormalize operators involving explicitly only light-quark degrees of freedom [5, 12]. At low-momentum scales, a virtual pair lives a sufficiently long time to permit the formation of strange hadronic components (e.g., a  $K\Lambda$  pair) of the nucleon wavefunction [13]. While this division between “extrinsic” and “intrinsic” strangeness is not rigorous, it does provide

a qualitative picture which suggests different approaches to estimating nucleon strange matrix elements.

In this note we consider intrinsic strangeness contributions to the matrix elements  $\langle N|\bar{s}\Gamma s|N\rangle$  ( $\Gamma = 1, \gamma_\mu, \gamma_\mu\gamma_5$ ) arising from kaon-strange baryon loops. Our calculation is intended to complement pole [14] and Skyrme [15] model estimates as well as to quantify the simple picture of nucleon strangeness arising from a kaon cloud. Although loop estimates have been carried out previously [16, 17], ours differs from others in several respects. First, we assume that nucleon electromagnetic (EM) and weak neutral current (NC) form factors receive contributions from a variety of sources (*e.g.*, loops and poles), so we make no attempt to adjust the input parameters to reproduce known form factors (*e.g.*,  $G_E^n$ ). Rather, we take our inputs from independent sources, such as fits to baryon-baryon scattering and quark model estimates where needed. We compute pion loop contributions to the nucleon's EM form factors using these input parameters and compare with the experimental values. Such a comparison provides an indication of the extent to which loops account for nucleon form factor physics generally and strangeness form factors in particular. Second, we employ hadronic form factors at the meson nucleon vertices and introduce "seagull" terms in order to satisfy the Ward-Takahashi (WT) Identity in the vector current sector. Previous loop calculations employed either a momentum cut-off in the loop integral [16] or meson-baryon form factor [17] but did not satisfy the WT Identity. We find that failure to satisfy the requirements of gauge invariance at this level can significantly alter one's results. Finally, we include an estimate of the strange quark scalar density which was not included in previous work.

## 2. The calculation.

The loop diagrams which we compute are shown in Fig. 1. In the case of vector current matrix elements, all four diagrams contribute, including the two seagull graphs (Fig. 1c,d) required by gauge invariance. For axial vector matrix elements, only the loop of Fig. 1a contributes, since  $\langle M|J_{\mu 5}|M\rangle \equiv 0$  for  $M$  a

pseudoscalar meson. The loops 1a and 1b contribute to  $\langle N|\bar{s}s|N\rangle$ . In a world of point hadrons satisfying SU(3) symmetry, the coupling of the lowest baryon and meson octets is given by

$$i\mathcal{L}_{BBM} = D \text{Tr}[(B\bar{B} + \bar{B}B)M] + F \text{Tr}[(B\bar{B} - \bar{B}B)M] \quad (1)$$

where  $\sqrt{2}B = \sum_a \psi_a \lambda_a$  and  $\sqrt{2}M = \sum_a \phi_a \lambda_a$  give the octet of baryon and meson fields, respectively, and where  $D + F = \sqrt{2}g_{\pi NN} = 19.025$  and  $D/F = 1.5$  according to Ref. [18]. Under this parameterization, one has  $g_{NEK}/g_{NAK} = \sqrt{3}(F - D)/(D + 3F) \approx -1/5$ , so that loops having an intermediate  $K\Sigma$  state ought to be generically suppressed by a factor of  $\sim 25$  with respect to  $K\Lambda$  loops. Analyses of  $K + N$  "strangeness exchange" reactions, however, suggest a serious violation of this SU(3) prediction [19], and imply that neglect of  $K\Sigma$  loops is not necessarily justified. Nevertheless, we consider only  $K\Lambda$  loops since we are interested primarily in arriving at the order of magnitude and qualitative features of loop contributions and not definitive numerical predictions.

With point hadron vertices, power counting implies that loop contributions to the mean square charge radius and magnetic moment are U.V. finite. In fact, the pion loop contributions to the nucleon's EM charge radius and magnetic moment have been computed previously in the limit of point hadron vertices [20]. Loop contributions to axial vector and scalar density matrix elements, however, are U.V. divergent, necessitating use of a cut-off procedure. To this end, we employ form factors at the meson-nucleon vertices used in determination of the Bonn potential from  $BB'$  scattering ( $B$  and  $B'$  are members of the lowest-lying baryon octet) [18]:

$$g_{NNM}\gamma_5 \longrightarrow g_{NNM}F(k^2)\gamma_5, \quad (2)$$

where

$$F(k^2) = \left[ \frac{m^2 - \Lambda^2}{k^2 - \Lambda^2} \right], \quad (3)$$

with  $m$  and  $k$  being the mass and momentum, respectively, of the meson. The Bonn values for cut-off  $\Lambda$  are typically in the range of 1 to 2 GeV. We note that this form reproduces the point hadron coupling for on-shell mesons ( $F(m^2) = 1$ ). An artifact of this choice is the vanishing of the form factors (and all loop amplitudes) for  $\Lambda = m$ . Consequently, when analyzing the  $\Lambda$ -dependence of our results below, we exclude the region about  $\Lambda = m$  as unphysical.

For  $\Lambda \rightarrow \infty$  (point hadrons), the total contribution from diagrams 1a and 1b to vector current matrix elements satisfies the WT Identity  $q^\mu \Lambda(p, p')_\mu = Q[\Sigma(p') - \Sigma(p)]$ , where  $Q$  is the nucleon charge associated with the corresponding vector current (EM, strangeness, baryon number, *etc*). For finite  $\Lambda$ , however, this identity is not satisfied by diagrams 1a+1b alone; inclusion of seagull diagrams (1c,d) is required in order to preserve it. To arrive at the appropriate seagull vertices, we treat the momentum-space meson-nucleon vertex functions as arising from a phenomenological lagrangian

$$i\mathcal{L}_{BBM} \longrightarrow g_{BBM} \bar{\psi} \gamma_5 \psi F(-\partial^2) \phi, \quad (4)$$

where  $\psi$  and  $\phi$  are baryon and meson fields, respectively. The gauge invariance of this lagrangian can be maintained via minimal substitution. We replace the derivatives in the d'Alembertian by covariant derivatives, expand  $F(-D^2)$  in a power series, identify the terms linear in the gauge field, express the resulting series in closed form, and convert back to momentum space. With our choice for  $F(k^2)$ , this procedure leads to the seagull vertex

$$-ig_{BBM} Q F(k^2) \left[ \frac{(q \pm 2k)_\mu}{(q \pm k)^2 - \Lambda^2} \right] \quad (5)$$

where  $q$  is the momentum of the gauge boson and where the upper (lower) sign corresponds to an incoming (outgoing) meson of charge  $Q$  (details of this procedure are given in Ref. [21]). With these vertices in diagrams 1c,d, the WT Identity in the presence of meson nucleon form factors is restored. We note that this prescription for satisfying gauge invariance is not unique; the specific underlying dynamics which give rise to  $F(k^2)$  could generate additional seagull terms

whose contributions independently satisfy the WT Identity. Indeed, different models of hadron structure may lead to meson-baryon form factors having a different form than our choice. However, for the purposes of our calculation, whose spirit is to arrive at order of magnitude estimates and qualitative features, the use of the Bonn form factor plus minimal substitution is sufficient.

The strange vector, axial vector, and scalar density couplings to the intermediate hadrons can be obtained with varying degrees of model-dependence. Since we are interested only in the leading  $q^2$ -behavior of the nucleon matrix elements as generated by the loops, we employ point couplings to the intermediate meson and baryon. For the vector currents, one has  $\langle \Lambda(p') | \bar{s} \gamma_\mu s | \Lambda(p) \rangle = f_V \bar{U}(p') \gamma_\mu U(p)$  and  $\langle K^0(p') | \bar{s} \gamma_\mu s | K^0(p) \rangle = \tilde{f}_V (p + p')_\mu$  with  $f_V = -\tilde{f}_V = 1$  in a convention where the  $s$ -quark has strangeness charge +1. The vector couplings are determined simply by the net strangeness of the hadron, independent of the details of any hadron model.

In the case of the axial vector, only the baryon coupling is required since pseudoscalar mesons have no diagonal axial vector matrix elements. Our approach in this case is to use a quark model to relate the “bare” strange axial vector coupling to the  $\Lambda$  to the bare isovector axial vector matrix element of the nucleon, where by “bare” we mean that the effect of meson loops has not been included. We then compute the loop contributions to the ratio

$$\eta_s = \frac{G_\Lambda^{(s)}(0)}{g_A}, \quad (6)$$

where  $G_\Lambda^{(s)}(q^2)$  is the strange quark axial vector form factor (see Eq. (10) below) and  $g_A = 1.262$  [22] is the proton's isovector axial vector form factor at zero momentum transfer. Writing  $\langle \Lambda(p') | \bar{s} \gamma_\mu \gamma_5 s | \Lambda(p) \rangle = f_A^0 \bar{U}(p') \gamma_\mu \gamma_5 U(p)$ , one has in the quark model  $f_A^0 = \int d^3x (u^2 - \frac{1}{3}\ell^2)$ , where  $u$  ( $\ell$ ) are the upper (lower) components of a quark in its lowest energy configuration [23, 24, 25]. The quark model also predicts that  $g_A^0 \equiv \frac{2}{3} \int d^3x (u^2 - \frac{1}{3}\ell^2)$ . In the present calculation, we take the baryon octet to be SU(3) symmetric (*e.g.*,  $m_N = m_\Lambda$ ), so that the quark

wavefunctions are the same for the nucleon and  $\Lambda$ .<sup>2</sup> In this case, one has  $f_A^0 = \frac{1}{2}g_A^0$ . This relation holds in both the relativistic quark model and the simplest non-relativistic quark model in which one simply drops the lower component contributions to the quark model integrals. We will make the further assumption that pseudoscalar meson loops generate the dominant renormalization of the bare axial couplings. The  $\Lambda$  has no isovector axial vector matrix element, while loops involving  $K\Sigma$  intermediate states are suppressed in the SU(3) limit as noted earlier. Under this assumption, then, only the  $\pi N$  loop renormalizes the bare coupling, so that  $g_A = g_A^0[1 + \Delta_A^\pi(\Lambda)]$ , where  $\Delta_A^\pi(\Lambda)$  gives the contribution from the  $\pi N$  loop with the bare coupling to the intermediate nucleon scaled out. In this case, the ratio  $\eta_s$  is essentially independent of the actual numerical predictions for  $f_A^0$  and  $g_A^0$  in a given quark model; only the spin-flavor factor  $\frac{1}{2}$  which relates the two enters.

For the scalar density, we require point couplings to both the intermediate baryon and meson. We write these couplings as  $\langle B(p')|\bar{q}q|B(p)\rangle = f_s^0 \bar{U}(p')U(p)$  and  $\langle M(p')|qq|M(p)\rangle = \gamma_M$ , where  $B$  and  $M$  denote the meson and baryon, respectively. Our choices for  $f_s^0$  and  $\gamma_M$  carry the most hadron model-dependence of all our input couplings. To reduce the impact of this model-dependence on our result, we again compute loop contributions to a ratio, namely,

$$R_s \equiv \frac{\langle N|\bar{s}s|N\rangle}{\langle N|\bar{u}u + \bar{d}d + \bar{s}s|N\rangle} \quad (7)$$

In the language of Ref. [2], one has  $R_s = y/(2+y)$ . Our aim in the present work is to compute  $R_s$  in a manner as free as possible from the assumptions made in extracting this quantity from standard  $\Sigma$ -term analyses. We therefore use the quark model to compute  $f_s^0$  and  $\gamma_M$  rather than obtaining these parameters from a chiral SU(3) fit to hadron mass splittings. We explore this alternative procedure, along with the effects of SU(3)-breaking in the baryon octet, elsewhere [21].

In the limit of good SU(3) symmetry for the baryon octet, the bare  $\bar{s}s$  matrix element of the  $\Lambda$  is  $f_s^0 = \int d^3x(u^2 - \ell^2)$ . Using the wavefunction normalization

<sup>2</sup>We investigate the consequences of SU(3)-breaking in the baryon octet in a forthcoming publication [21]

condition  $\int d^3x(u^2 + \ell^2) = 1$ , together with the quark model expression for  $g_A^0$ , leads to

$$f_s^0 = \frac{1}{2}(\frac{1}{2}g_A^0 - 1) \quad (8)$$

Neglecting loops, one has  $\langle N|\bar{u}u + \bar{d}d + \bar{s}s|N\rangle = 3f_s^0$ . We include loop contributions to both the numerator and denominator of Eq. (7). Although the latter turn out to be numerically unimportant, their inclusion guarantees that  $R_s$  is finite in the chiral limit.

Were the contribution from Fig. 1a dominant, the loop estimate of  $R_s$  would be nearly independent of  $f_s^0$ . The contribution from Fig. 1b, however, turns out to have comparable magnitude. Consequently, we are unable to minimize the hadron model-dependence in our estimate of  $R_s$  to the same extent as with  $\eta_s$  and the vector current form factors. To arrive at a value for  $f_s^0$ , we consider three alternatives: (A) Compute  $f_s^0$  using the MIT bag model value for  $g_A^0$  and use a cut-off  $\Lambda \sim \Lambda_{\text{Bonn}}$  in the meson-baryon form factor. This scenario suffers from the conceptual ambiguity that the Bonn value for the cut-off mass in  $F(k^2)$  allows for virtual mesons of wavelength smaller than the bag radius. (B) Compute  $f_s^0$  as in (A) and take the cut-off  $\Lambda \sim 1/R_{\text{bag}}$ . This approach follows in the spirit of so-called “chiral quark models”, such as that used in the calculation of Ref. [17], which assume the virtual pseudoscalar mesons are Goldstone bosons that live only outside the bag and couple directly to the quarks at the bag surface. While conceptually more satisfying than (A), this choice leads to a form factor  $F(k^2)$  inconsistent with  $BB'$  scattering data. (C) First, determine  $g_A^0$  assuming pion-loop dominance in the isovector axial form factor, i.e.,  $g_A = g_A^0[1 + \Delta_A^\pi(\Lambda)]$ . Second, use this value of  $g_A^0$  to determine  $f_s^0$  via Eq. (8). Surprisingly, this procedure yields a value for  $g_A^0$  very close to the MIT bag model value for  $\Lambda \sim \Lambda_{\text{Bonn}}$  rather than  $\Lambda \sim 1/R_{\text{bag}}$  as one might naively expect.

Since all three of these scenarios are consistent with the bag estimate for  $g_A^0$  (and renormalization constant,  $Z$  as discussed below) we follow the “improved bag” procedure of Ref. [24] to obtain  $\gamma_M$ . The latter gives  $\gamma_M \equiv$

$\langle M(p')|\bar{q}q|M(p)\rangle = 1A/R$ , where  $R$  is the bag radius for meson  $M$ . Using  $R_\pi \approx R_K \approx 3.5 \text{ GeV}^{-1}$ , one has  $\gamma_\pi \approx \gamma_K \approx 0.4 \text{ GeV}$ . This procedure involves a certain degree of theoretical uncertainty. The estimate for  $\gamma_K$  ( $\gamma_\pi$ ) is obtained by expanding the bag energy to leading non-trivial order in  $m_K$  and  $m_\pi$  ( $m_\pi$  and  $m_{u,d}$ ), and we have at present no estimate of the corrections induced by higher-order terms in these masses.

Using the above couplings, we compute the kaon loop contributions to the strange quark scalar density as well as vector and axial vector form factors. The latter are defined as

$$\langle N(p')|J_\mu(0)|N(p)\rangle = \bar{U}(p')\left[F_1\gamma_\mu + \frac{iF_2}{2m_N}\sigma_{\mu\nu}q^\nu\right]U(p) \quad (9)$$

$$\langle N(p')|J_{\mu 5}(0)|N(p)\rangle = \bar{U}(p')\left[G_A\gamma_\mu + G_P\frac{q_\mu}{m_N}\right]\gamma_5 U(p) \quad (10)$$

where  $J_\mu$  is either the EM or strange quark vector current and  $J_{\mu 5}$  is the strange axial vector current. The induced pseudoscalar form factor,  $G_P$ , does not enter semi-leptonic neutral current scattering processes at an observable level, so we do not discuss it here. In the case of the EM current, pion loop contributions to the neutron form factors arise from the same set of diagrams as contribute to the strange vector current matrix elements but with the replacements  $K^0 \rightarrow \pi^-$ ,  $\Lambda \rightarrow n$ , and  $g_{NAK} \rightarrow \sqrt{2}g_{\pi NN}$ . For the proton, one has a  $\pi^0$  in Fig. 1a and a  $\pi^+$  in Figs. 1b-d. We quote results for both Dirac and Pauli form factors as well as for the Sachs electric and magnetic form factors [26], defined as  $G_E = F_1 - \tau F_2$  and  $G_M = F_1 + F_2$ , respectively, where  $\tau = -q^2/4m_N^2$  and  $q^2 = \omega^2 - |\vec{q}|^2$ . We define the magnetic moment as  $\mu = G_M(0)$  and dimensionless mean square Sachs and Dirac charge radii (EM or strange) as

$$\rho^{\text{sachs}} = \frac{dG_E(\tau)}{d\tau}\bigg|_{\tau=0} \quad (11)$$

$$\rho^{\text{dirac}} = \frac{dF_1(\tau)}{d\tau}\bigg|_{\tau=0} \quad (12)$$

The dimensionless radii are related to the dimensionful mean square radii by  $\langle r^2 \rangle_{\text{sachs}} = 6 \, dG_E/dq^2 = -(3/2m_N^2)\rho^{\text{sachs}}$  and similarly for the corresponding

Dirac quantities. From these definitions, one has  $\rho^{\text{dirac}} = \rho^{\text{sachs}} + \mu$ . To set the scales, we note that the Sachs EM charge radius of the neutron is  $\rho_n^{\text{sachs}} \approx -\mu_n$ , corresponding to an  $\langle r_n^2 \rangle_{\text{sachs}}$  of about  $-0.13 \text{ fm}^2$ . Its Dirac EM charge radius, on the other hand, is nearly zero. We note also that it is the Sachs, rather than the Dirac, mean square radius which characterizes the spatial distribution of the corresponding charge inside the nucleon, since it is the combination  $F_1 - \tau F_2$  which arises naturally in a non-relativistic expansion of the time component of Eq. (9).

### 3. Results and discussion

Our results are shown in Fig. 2, where we plot the different strange matrix elements as a function of the form factor cut-off,  $\Lambda$ . Although we quote results in Table I corresponding to the Bonn fit values for  $\Lambda$ , we show the  $\Lambda$ -dependence away from  $\Lambda_{\text{Bonn}}$  to indicate the sensitivity to the cut-off. In each case, we plot two sets of curves corresponding, respectively, to  $m = m_K$  and  $m = m_\pi$ , in order to illustrate the dependence on meson mass as well as to show the pion loop contributions to the EM form factors. The dashed curves for the mean square radius and magnetic moment give the values for  $\Lambda \rightarrow \infty$ , corresponding to the point hadron calculation of Ref. [20]. We reiterate that the zeroes arising at  $\Lambda = m$  are an unphysical artifact of our choice of nucleon-meson form factor, and one should not draw conclusions from the curves in the vicinity of these points.

In order to interpret our results, it is useful to refer to the analytic expressions for the loops in various limits. The full analytic expressions will appear in a forthcoming publication [21]. In the case of the vector current form factors, the use of monopole meson-nucleon form factor plus minimal substitution leads to the result that

$$F_{(i)}(q^2) = F_{(i)}^{\text{point}}(m^2; q^2) - F_{(i)}^{\text{point}}(\Lambda^2; q^2) + (\Lambda^2 - m^2) \frac{d}{d\Lambda^2} F_{(i)}^{\text{point}}(\Lambda^2; q^2) \quad (13)$$

where  $F_{(i)}^{\text{point}}(m^2; q^2)$  is the point hadron result of Ref. [20] for loops with meson of mass  $m$ . It is straightforward to show that the  $\Lambda$ -dependent terms in Eq. (13)

vanish in the  $\Lambda \rightarrow \infty$  limit, thereby reproducing the point hadron result. For finite cut-off, the first few terms in a small- $m^2$  expansion of the radii and magnetic moment are given by

$$\rho^{\text{sachs}} = -\frac{1}{3} \left( \frac{g}{4\pi} \right)^2 (3 - 5\bar{m}^2) \ln \frac{m^2}{\Lambda^2} + \dots \quad (14)$$

$$\rightarrow \left( \frac{g}{4\pi} \right)^2 \left[ 2 - \frac{1}{3} (3 - 5\bar{m}^2) \ln \frac{m^2}{m_N^2} + \dots \right]$$

$$\rho^{\text{dirac}} = -\frac{1}{3} \left( \frac{g}{4\pi} \right)^2 (3 - 8\bar{m}^2) \ln \frac{m^2}{\Lambda^2} + \dots \quad (15)$$

$$\rightarrow -\frac{1}{3} \left( \frac{g}{4\pi} \right)^2 (3 - 8\bar{m}^2) \ln \frac{m^2}{m_N^2} + \dots$$

$$\mu = \left( \frac{g}{4\pi} \right)^2 \bar{m}^2 \ln \frac{m^2}{\Lambda^2} + \dots \rightarrow \left( \frac{g}{4\pi} \right)^2 \left[ -2 + \bar{m}^2 \ln \frac{m^2}{m_N^2} + \dots \right] \quad (16)$$

where  $\bar{m} \equiv m/m_N$ . Taking  $m = m_\pi$  and  $g = \sqrt{2}g_{\pi NN}$  gives the neutron EM charge radii and magnetic moment, while setting  $m = m_K$  and  $g = g_{NAK}$  gives the strangeness radius and magnetic moment. The expressions to the right of the arrows give the first few terms in a small- $m^2$  expansion in the  $\Lambda \rightarrow \infty$  limit. The cancellation in this limit of the logarithmic dependence on  $\Lambda$  arises from terms not shown explicitly ( $+\dots$ ) in Eqs. (14-16).

In the case of the axial form factor, we assume the pseudoscalar meson loops to give the dominant correction to the bare isovector axial matrix element of the nucleon. This assumption may be more justifiable than in the case of the vector current form factors, since the lightest pseudovector isovector and isoscalar mesons which can couple to the nucleon are the  $a_1(1260)$  and  $f_1(1285)$ , respectively. In this case one has  $g_A^{\text{phys}} \approx g_A^0 [1 + \Delta_A^*]$  and  $\eta_s \approx \frac{1}{3} \Delta_A^* / [1 + \Delta_A^*]$  where the  $\frac{1}{3}$  is just the spin-flavor factor relating  $f_A^0$  and  $g_A^0$ . The loop contributions are given by the  $\Delta_A^{*,K}$ , where

$$\Delta_A^{*,\pi} = \pm \left( \frac{g}{4\pi} \right)^2 \left[ \frac{\bar{\Lambda}^2}{3} \left( \frac{\bar{m}^2 - \bar{\Lambda}^2}{4 - \bar{\Lambda}^2} \right) + \frac{1}{4} (2\bar{m}^2 - \bar{\Lambda}^2) \ln \bar{\Lambda}^2 + \dots \right] \quad (17)$$

$$\rightarrow \pm \left( \frac{g}{4\pi} \right)^2 \left[ -\frac{1}{2} \ln \bar{\Lambda}^2 + \frac{5}{4} + \frac{1}{2} \bar{m}^2 + \dots \right] \quad (18)$$

where  $g = g_{NAK}$  or  $g_{\pi NN}$  as appropriate, and where  $\bar{\Lambda} = \Lambda/m_N$ . The upper (lower) sign corresponds to the kaon (pion) loop. The opposite sign arises from the fact that  $\Delta_A^*$  receives contributions from two loops, corresponding to a neutral and charged pion, respectively. The isovector axial vector coupling to the intermediate nucleon in these loops ( $n$  and  $p$ ) have opposite signs, while the  $\pi^\pm$ -loop carries an additional factor of two due to the isospin structure of the  $NN\pi$  vertex.

For the scalar density, we obtain  $R_s = \tilde{\Delta}_s^K / [3f_s + \Delta_s^K + \Delta_s^*]$ , where the loop contributions are contained in

$$\tilde{\Delta}_s^K = \left( \frac{g_{NAK}}{4\pi} \right)^2 \left[ f_s F_s^a(m_K, \Lambda) + \bar{\gamma}_K F_s^b(m_K, \Lambda) \right] \quad (19)$$

$$\Delta_s^K = \left( \frac{g_{NAK}}{4\pi} \right)^2 \left[ 3f_s F_s^a(m_K, \Lambda) + 2\bar{\gamma}_K F_s^b(m_K, \Lambda) \right] \quad (20)$$

and  $\Delta_s^*$ , where the expression for the latter is the same as that for  $\Delta_s^K$  but with the replacements  $\bar{\gamma}_K \rightarrow \bar{\gamma}_\pi$ ,  $m_K \rightarrow m_\pi$ , and  $g_{NAK} \rightarrow \sqrt{3}g_{\pi NN}$ , and where  $\bar{\gamma}_{\pi,K} = \gamma_{\pi,K}/m_N$ . The functions  $F_s^a$  and  $F_s^b$ , which represent the contributions from loops 1a (baryon insertion) and 1b (meson insertion), respectively, are given by

$$F_s^a(m, \Lambda) = 2 \left( \frac{\bar{\Lambda}^2 - \bar{m}^2}{4 - \bar{\Lambda}^2} \right) + \frac{1}{2} \bar{m}^2 \ln \frac{m^2}{\Lambda^2} + \dots \quad (21)$$

$$\rightarrow \ln \bar{\Lambda}^2 - 2 + \frac{1}{2} \bar{m}^2 \ln \bar{m}^2 + \dots$$

$$F_s^b(m, \Lambda) = 1 - \frac{1}{2} \left( \frac{\bar{\Lambda}^2 \bar{m}^2 - \bar{m}^2 - \bar{\Lambda}^2}{\bar{\Lambda}^2 - \bar{m}^2} \right) \ln \frac{m^2}{\Lambda^2} + \dots \quad (22)$$

$$\rightarrow 1 + \frac{1}{2} (1 - \bar{m}^2) \ln \bar{m}^2 + \dots$$

The expressions in Eqs. (14-22) and curves in Fig. 2 lend themselves to a number of observations. Considering first the vector and axial vector form factors, we note that the mean-square radii display significant SU(3)-breaking. The loop contributions to the radii contain an I.R. divergence associated with the meson mass which manifests itself as a leading chiral logarithm in Eqs. (14-15). The effect is especially pronounced for  $\rho^{\text{dirac}}$ , where, for  $\Lambda > 1$  GeV, the

results for  $m = m_\pi$  are roughly an order of magnitude larger than the results for  $m = m_K$  (up to overall sign). In contrast, the scale of SU(3)-breaking is less than a factor of three for the magnetic moment and axial form factor over the same cut-off range. The chiral logarithms which enter the latter quantities are suppressed by at least one power of  $\bar{m}^2$ , thereby rendering these quantities I.R. finite and reducing the impact of SU(3)-breaking associated with the meson mass. Consequently, in a world where nucleon strange-quark form factors arose entirely from pseudoscalar meson loops, one would see a much larger strangeness radius (commensurate with the neutron EM charge radius) were the kaon as light as the pion than one would see in the actual world. The scales of the strange magnetic moment and axial form factor, on the other hand, would not be appreciably different with a significantly lighter kaon.

From a numerical standpoint, the aforementioned qualitative features have some interesting implications for present and proposed experiments. Taking the meson-nucleon form factor cut-off in the range determined from fits to  $BB'$  scattering,  $1.2 \leq \Lambda_{\text{Donn}} \leq 1.4$  GeV, we find  $\mu_s$  has roughly the same scale as the nucleon's isoscalar EM magnetic moment,  $\mu^{I=0} = \frac{1}{2}(\mu_p + \mu_n)$ . The loop contribution is comparable in magnitude and has the same sign as pole [14] and Skyrme [15] predictions. While the extent to which the loop and pole contributions are independent and ought to be added is open to debate, the scale of these two contributions, as well as the Skyrme estimate, point to a magnitude for  $\mu_s$  that ought to be observable in the SAMPLE experiment [6] and the  $G^0$  experiment [8]. Similarly, the loop and Skyrme estimates for  $\eta_s$  agree in sign and rough order of magnitude, the latter being about half the value extracted from the  $\nu p/\bar{\nu} p$  cross sections [3]. Under the identification of the strange-quark contribution to the proton's spin  $\Delta s$  with  $G_A^{(s)}(0)$ , one finds a similar experimental value for  $\eta_s$  from the EMC data [4].

In contrast, predictions for the strangeness radius differ significantly between the models. In the case of the Sachs radius, the signs of the loop and pole predictions differ. The sign of loop predictions corresponds to one's naive expectation

that the kaon, having negative strangeness, exists further from the center of the  $K - \Lambda$  system due to its lighter mass. Hence, one would expect a positive value for  $\rho_s^{\text{sachs}}$  (recall that  $\rho_s^{\text{sachs}}$  and  $\langle r^2 \rangle_{\text{sachs}}$  have opposite signs). The magnitude of the loop prediction for  $\rho_s^{\text{sachs}}$  is roughly 1/4 to 1/3 that of the pole and Skyrme models and agrees in sign with the latter. In the case of the Dirac radius, the loop contribution is an order of magnitude smaller than either of the other estimates. From the standpoint of measurement, we note that a low- $|q^2|$ , forward-angle measurement of the elastic  $\bar{e}p$  PV asymmetry,  $A_{LR}(\bar{e}p)$ , is sensitive to the combination  $\rho_s^{\text{sachs}} + \mu_p \mu_s$  [28]. The asymmetry for scattering from a  $(J^\pi, I) = (0^+, 0)$  nucleus such as  $^4\text{He}$ , on the other hand, is sensitive primarily to the Sachs radius [28]. Thus, were the kaon cloud to be the dominant contributor to the nucleon's vector current strangeness matrix elements, one would not be able to observe them with the forward-angle  $A_{LR}(\bar{e}p)$  measurements of Refs. [7,8], whereas one potentially could do so with the  $A_{LR}(^4\text{He})$  measurements of Refs. [7,9]. Were the pole or Skyrme models reliable predictors of  $\langle N | s \gamma_\mu s | N \rangle$ , on the other hand, the strangeness radii (Dirac and/or Sachs) would contribute at an observable level to both types of PV asymmetry. As we illustrate elsewhere [21], the scale of the pole prediction is rather sensitive to one's assumptions about the asymptotic behavior of the vector current form factors; depending on one's choice of conditions, the pole contribution could be significantly smaller in magnitude than prediction of Ref. [14]. Given these results, including the difference in sign between the pole and both the loop and Skyrme estimates, a combination of PV asymmetry measurements on different targets could prove useful in determining which picture gives the best description of nucleon's vector current strangeness content.

From Eqs.(19-22), one has that the loop contributions to the scalar density contain both U.V. and chiral singularities. The U.V. divergence arises from the  $\bar{q}q$  insertion in the intermediate baryon line, while the chiral singularity appears in the loop containing the scalar density matrix element of the intermediate meson. Despite the chiral singularity, loop contributions to the matrix elements  $m_q \langle N | \bar{q}q | N \rangle$  are finite in the chiral limit due to the pre-multiplying factor of



$m_q$ . The ratio  $R_s$  is also well-behaved in this limit as well as in the limit of large  $\Lambda$ . For  $m_\pi \rightarrow 0$  and  $m_K \rightarrow 0$  simultaneously, one has  $R_s \sim 1/8$ , while for  $\Lambda \rightarrow \infty$ , the ratio approaches  $1/12$ . These limiting values are independent of the couplings  $f_s$  and  $\gamma_{\pi,K}$  and are determined essentially by counting the number of logarithmic singularities (U.V. or chiral) entering the numerator and denominator of  $R_s$  (note that we have not included  $\eta$  loops in this analysis). Consequently, the values for  $R_s$  in the chiral and infinite cut-off limits do not suffer from the theoretical ambiguities encountered in the physical regime discussed in Section 2. It is also interesting to observe that the limiting results have the same sign and magnitude as the value of  $R_s$  extracted from the  $\Sigma$ -term.

For  $\Lambda \leq \Lambda_{\text{Donn}}$  and for  $m_\pi$  and  $m_K$  having their physical values, the prediction for  $R_s$  is smaller than in either of the aforementioned limits and rather dependent on the choice of  $f_s^0$  and  $\gamma_M$ . The sensitivity to the precise numerical values taken by these couplings is magnified by a phase difference between  $F_s^a$  and  $F_s^b$ . The range of results associated with scenarios (A)-(C) is indicated in Table I, with the largest values arising from choices (A) and (C). The change in overall sign arises from the sign difference between loops 1a and 1b and the increasing magnitude of  $F_s^b$  relative to  $F_s^a$  as  $\Lambda$  becomes small. These results are suggestive that loops may give an important contribution to the nucleon's strange-quark scalar density, though the predictive power of the present estimate is limited by the sensitivity to the input couplings. We emphasize, however, that our estimates of the vector and axial vector form factors do not manifest this degree of sensitivity.

We note in passing that scenario (C) gives a value for  $\mathfrak{F}_A^0 = g_A[1 + \Delta_A^*(\Lambda)]^{-1} \approx g_A^0(\text{bag})$  for  $\Lambda \sim \Lambda_{\text{Donn}}$ . The value obtained for  $g_A^0$  in this case depends only on the assumption that pseudoscalar meson loops give the dominant correction to  $g_A^0$  and involves no statements about the details of quark model wavefunctions. In contrast, for  $\Lambda \sim 1/R_{\text{bag}}$  we find  $g_A^0 \approx g_A$ . We also note that scenarios (A) and (C) are consistent with the bag value for the scalar density renormalization factor,  $Z$ . The latter is defined as  $Z = \langle H | \bar{q}q | H \rangle / N_q$ , where  $N_q$  is the number of valence quarks in hadron  $H$  [24, 27]. A test of consistency, then, is the extent

to which the equality  $f_s^0 = Z$  is satisfied. When  $f_s^0$  is computed using Eq. (8), we find  $f_s^0 \approx 0.5$  in scenarios (A) and (C), while one has  $Z_{\text{bag}} \approx 0.5$  [24]. These statements would seem to support the larger values for  $R_s$  in Table I.

As for the  $\Lambda$ -dependence of the form factors, we find that the radii do not change significantly in magnitude over the range  $\Lambda_{\text{Donn}} \leq \Lambda \leq \infty$ , owing in part to the importance of the chiral logarithm. The variation in the magnetic moment, whose chiral logarithm is suppressed by a factor of  $\bar{m}^2$ , is somewhat greater (about a factor of four for  $m = m_K$ ). The ratio  $\eta_s$  is finite as  $\Lambda \rightarrow \infty$ , with a value of  $\approx -3/5$  in this limit. This limit is approached only for  $\Lambda \gg$  the range of values shown in Fig. 2d, so we do not indicate it on the graph. The I.R. divergence ( $\Lambda \ll 1 \text{ fm}^{-1}$ ) in the vector current quantities is understandable from Eq. (13), which has the structure of a generalized Pauli-Villars regulator. The impact of the monohole meson-nucleon form factor is similar to that of including additional loops for a meson of mass  $\Lambda$ . From the I.R. singularity in the radii associated with the physical meson, one would expect a similar divergence in  $\Lambda$ , but with opposite sign. The appearance of a singularity having the same sign as the chiral singularity, as well as the appearance of an I.R. divergence in the  $\Lambda$ -dependence of magnetic moment which displays no chiral singularity, is due to the derivative term in Eq. (13). In light of this strong  $\Lambda$ -dependence at very small values, as well as our philosophy of taking as much input from independent sources (*viz.*  $BB'$  scattering) we quote in Table 1 results for our loop estimates using  $\Lambda \sim \Lambda_{\text{Donn}}$ .

It is amusing, nonetheless, to compare our results for  $m = m_K$  and  $\Lambda \sim 1 \text{ fm}^{-1}$  with those of the calculation of Ref. [17], which effectively excludes contributions from virtual kaons having wavelength smaller than the nucleon size. Assuming this regime in the cut-off is sufficiently far from the artificial zero at  $\Lambda = m_K$  to be physically meaningful, our result for  $\eta_s$  agrees in magnitude and sign with that of Ref. [17]. In contrast, our estimates are about a factor of three larger for the strangeness radii and a factor of seven larger for the strange magnetic moment. We suspect that this disagreement is due, in part, to the different treatment of

gauge invariance in the two calculations. In the case of the axial vector form factor, which receives no seagull contribution, the two calculations agree. Had we omitted the seagull contributions, our results for the Sachs radius would also have agreed. For the Dirac radius our estimate would have been three times smaller and for the magnetic moment three times larger than the corresponding estimates of Ref. [17]. At  $\Lambda \sim \Lambda_{\text{Bonn}}$ , the relative importance of the seagull for  $\rho_s^{\text{sachs}}$  and  $\mu_s$  is much smaller ( $\sim 30\%$  effect) than at small  $\Lambda$ , whereas omission of the seagull contribution to  $\rho_s^{\text{dirac}}$  would have reduced its value by more than an order of magnitude. We conclude that the extent to which one respects the requirements of gauge invariance at the level of the WT Identity can significantly affect the results for loops employing meson-nucleon form factors. We would argue that a calculation which satisfies the WT Identity is likely to be more realistic than one which doesn't and speculate, therefore, that the estimate of Ref. [17] represents an underestimate of the loop contributions to  $\rho_s$  and  $\mu_s$ . An attempt to perform a chiral-quark model calculation satisfying the WT Identity in order to test this speculation seems warranted.

Finally, we make two caveats as to the limit of our calculation's predictive power. First, we observe that for  $\Lambda \sim \Lambda_{\text{Bonn}}$ , the pion-loop gives a value for  $\mu_n$  very close to the physical value, but significantly over-estimates the neutron's EM charge radii, especially  $\rho_n^{\text{dirac}}$  (see Fig. 2b). One would conclude, then, that certainly in the case of mean-square radii, loops involving only the lightest pseudoscalar mesons do not give a complete account of low-energy nucleon form factor physics. Some combination of additional loops involving heavier mesons and vector meson pole contributions is likely to give a more realistic description of the strangeness vector current matrix elements. In this respect, the work of Ref. [29] is suggestive.

Second, had we adopted the heavy-baryon chiral perturbation framework of Ref. [30], we would have kept only the leading non-analytic terms in  $m$ , since in the heavy baryon expansion contributions of order  $m^p$ ,  $p = 1, 2, \dots$  are ambiguous. Removal of this ambiguity would require computing order  $m^p$  contributions

to a variety of processes in order to tie down the coefficients of higher-dimension operators in a chiral lagrangian. The present calculation, however, was not carried out within this framework and gives, in effect, a model for the contributions analytic in  $m$ . For  $m = m_\kappa$ , these terms contribute non-negligibly to our results. We reiterate that our aim is not so much to make reliable numerical predictions as to provide insight into orders of magnitude, signs, and qualitative features of nucleon strangeness. Were one interested in arriving at more precise numerical statements, even the use of chiral perturbation theory could be insufficient, since it appears from our results that pole and heavier meson loops are likely to give important contributions to the form factors. From this perspective, then, it makes as much sense to include terms analytic in  $m$  as to exclude them, especially if we are to make contact with the previous calculations of Refs. [16, 17, and 20].

In short, we view the present calculation as a baseline against which to compare future, more extensive loop analyses. Based on a simple physical picture of a kaon cloud, it offers a way, albeit provisional, of understanding how strange quark matrix elements of the nucleon might exist with observable magnitude, in spite of the success with which constituent quark models of the nucleon account for its other low-energy properties. At the same time, we have illustrated some of the qualitative features of loop contributions, such as the impact of SU(3)-breaking in the pseudoscalar meson octet, the sensitivity to one's form factor at the hadronic vertex, and the importance of respecting gauge invariance at the level of the WT Identity. Finally, when taken in tandem with the calculations of Refs. [14, 15], our results strengthen the rationale for undertaking the significant experimental investment required to probe nucleon strangeness with semi-leptonic scattering.

## ACKNOWLEDGEMENTS

It is a pleasure to thank S. J. Pollock, B. R. Holstein, W. C. Haxton, N. Isgur, and E. Lomon for useful discussions.

## REFERENCES

1. T.P. Cheng, *Phys. Rev. D* **13** (1976) 2161.
2. J. Gasser, H. Leutwyler, and M.E. Sainio, *Phys. Lett. B* **253** (1991) 252.
3. L.A. Ahrens *et al.*, *Phys. Rev. D* **35** (1987) 785.
4. J. Ashman *et al.*, *Nucl. Phys. B* **328** (1989) 1.
5. D. B. Kaplan and A. Manohar, *Nucl. Phys. B* **310** (1988) 527.
6. MIT-Bates proposal # 89-06, Bob McKeown and D. H. Beck, contact people.
7. CEBAF proposal # PR-91-010, J.M. Finn and P.A. Souder, spokespersons.
8. CEBAF proposal # PR-91-017, D.H. Beck, spokesperson.
9. CEBAF proposal # PR-91-004, E.J. Beise, spokesperson.
10. LAMPF Proposal # 1173, W.C. Louis, contact person.
11. S.J. Brodsky, P. Hoyer, C. Peterson, and N. Sakai, *Phys. Lett. B* **93** (1980) 451; S.J. Brodsky, C. Peterson, and N. Sakai, *Phys. Rev. D* **23** (1981) 2745.
12. J. Collins, F. Wilczek, and A. Zee, *Phys. Rev. D* **18** (1978) 242.
13. M. Burkardt and B.J. Warr, *Phys. Rev. D* **45** (1992) 958.
14. R. L. Jaffe, *Phys. Lett. B* **229** (1989) 275.
15. N. W. Park, J. Schechter and H. Weigel, *Phys. Rev. D* **43**, 869 (1991).
16. B.R. Holstein, in *Proceedings of the Caltech Workshop on Parity Violation in Electron Scattering*, E.J. Beise and R.D. McKeown, Eds., World Scientific (1990), pp. 27-43.
17. W. Koepf, E.M. Henley, and S.J. Pollock, *Phys. Lett. B* **288** (1992) 11.
18. B. Holzenkamp, K. Holinde, and J. Speth, *Nucl. Phys. A* **500** (1989) 485.
19. E. Hirsch *et al.*, *Phys. Lett. B* **36** (1971) 139; E. Hirsch, U. Karshon, and H.J. Lipkin, *Phys. Lett. B* **36** (1971) 385.
20. H.A. Bethe and F. delioffman, *Mesons and Fields* (Row, Peterson, and Co., Evanston, IL, 1955), Vol. II, p.289ff.
21. M.J. Musolf and M. Burkardt, to be published.
22. J.M. Gaillard and G. Sauvage, *Ann. Rev. Nuc. Part. Sci.* **34** (1984) 351; D. Dubbers, W. Mampe, and J. Döhner, *Europhys. Lett.* **11** (1990) 195; S. Freedman, *Comments Nucl. Part. Phys.* **19** (1990) 209; M. Bourquin *et al.*, *Z. für Phys. C* **21** (1983) 27.
23. A. Chodos, R.L. Jaffe, K. Johnson, and C.B. Thorn, *Phys. Rev. D* **10** (1974) 2599; T. DeGrand, R.L. Jaffe, K. Johnson, and J. Kiskis, *Phys. Rev. D* **12** (1975) 2060.
24. J.F. Donoghue and K. Johnson, *Phys. Rev. D* **21** (1980) 1975.
25. J.F. Donoghue, E. Golowich, and B.R. Holstein, *Phys. Rep.* **131** (1986) 319.
26. R.G. Sachs, *Phys. Rev.* **126** (1962) 2256.

27. S. Weinberg, in *Festschrift for I. I. Rabi*, edited by Lloyd Moltz (N. Y. Academy of Sciences, N.Y., 1977).
28. M.J. Musolf and T.W. Donnelly, *Nucl. Phys.* **A546** (1992) 509.
29. P. Geiger and N. Isgur, CEBAF Theory Pre-print #CEBAF-TH-92-24 (1992).
30. E. Jenkins and A.V. Manohar, *Phys. Lett.* **B255** (1991) 558.

### FIGURE CAPTIONS

**Fig. 1.** Feynman diagrams for loop contributions to nucleon strange quark matrix elements. Here,  $\otimes$  denotes insertion of the operator  $\bar{s}\Gamma s$  where  $\Gamma = 1, \gamma_\mu$ , or  $\gamma_\mu\gamma_5$ . All four diagrams contribute to vector current matrix elements. Only diagram 1a enters the axial vector matrix element. Both 1a and 1b contribute to the scalar density.

**Fig. 2.** Strange quark vector and axial vector parameters as a function of nucleon-meson form factor mass,  $\Lambda$ . Here,  $\rho_s$  denotes the dimensionless Sachs (2a) and Dirac (2b) strangeness radii. The strange magnetic moment is given in (2c). The axial vector ratio  $\eta_s$  is shown in (2d). Dashed curves indicate values of these parameters for  $\Lambda \rightarrow \infty$ . The ranges corresponding to the Bonn values for  $\Lambda$  are indicated by the arrows. The strong meson-nucleon coupling  $(g/4\pi)^2$  has been scaled out in (2a-c) and must multiply the results in Fig. 2 to obtain the values in Table I.

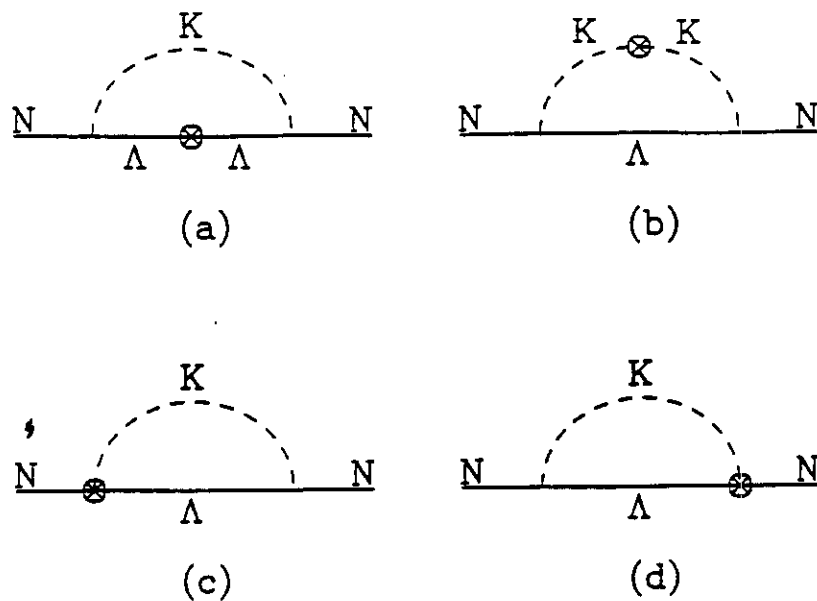


Fig. 1.

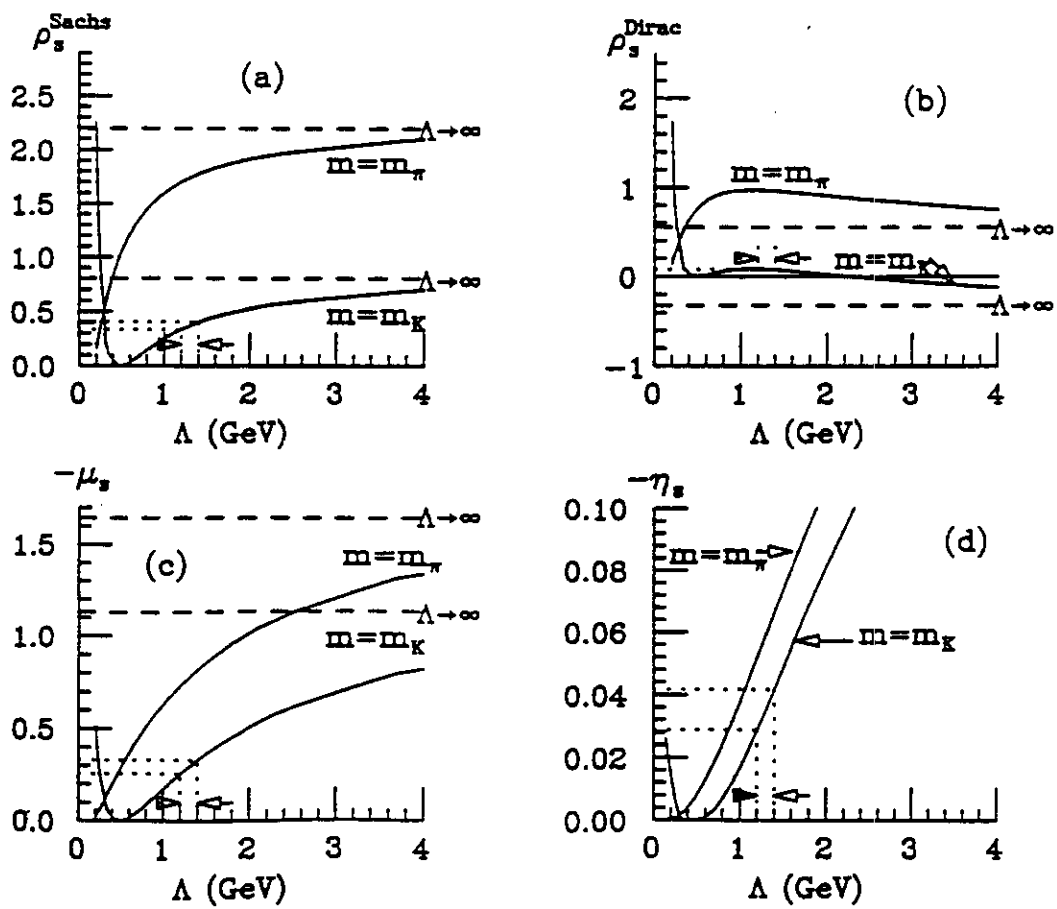


Fig. 2.